Proton transfer reaction mass spectrometry investigations of phthalate esters via direct headspace sampling

Olivenza-León, D., Mayhew, C. A. & González-Méndez, R.

Author post-print (accepted) deposited by Coventry University's Repository

Original citation & hyperlink:
Olivenza-León, D, Mayhew, CA & González-Méndez, R 2021, 'Proton transfer reaction mass spectrometry investigations of phthalate esters via direct headspace sampling', International Journal of Mass Spectrometry, vol. 461, 116497.
https://dx.doi.org/10.1016/j.ijms.2020.116497

DOI 10.1016/j.ijms.2020.116497
ISSN 1387-3806

Publisher: Elsevier

NOTICE: this is the author's version of a work that was accepted for publication in International Journal of Mass Spectrometry. Changes resulting from the publishing process, such as peer review, editing, corrections, structural formatting, and other quality control mechanisms may not be reflected in this document. Changes may have been made to this work since it was submitted for publication. A definitive version was subsequently published in International Journal of Mass Spectrometry, 461, (2021) DOI: 10.1016/j.ijms.2020.116497

© 2020, Elsevier. Licensed under the Creative Commons Attribution-NonCommercial-NoDerivatives 4.0 International
http://creativecommons.org/licenses/by-nc-nd/4.0/

Copyright © and Moral Rights are retained by the author(s) and/ or other copyright owners. A copy can be downloaded for personal non-commercial research or study, without prior permission or charge. This item cannot be reproduced or quoted extensively from without first obtaining permission in writing from the copyright holder(s). The content must not be changed in any way or sold commercially in any format or medium without the formal permission of the copyright holders.

This document is the author's post-print version, incorporating any revisions agreed during the peer-review process. Some differences between the published version and this version may remain and you are advised to consult the published version if you wish to cite from it.

Proton Transfer Reaction Mass Spectrometry Investigations of Phthalate Esters via Direct Headspace Sampling

David Olivenza-León,[1] Chris A. Mayhew[1,2] and Ramón González-Méndez[1,3*]

1. Molecular Physics Group, School of Physics and Astronomy, University of Birmingham, Edgbaston, Birmingham, B15 2TT, UK
2. Institut for Breath Research, University of Innsbruck, Rathausplatz 4, A-6850 Dornbirn, Austria
3. Centre for Agroecology, Water and Resilience, Coventry University, Coventry, CV1 5FB, UK

*Corresponding Author Tel.: +44 247 7651678.
E-mail: Ramon.Gonzalez-Mendez@coventry.ac.uk / R.GonzalezMendez@bham.ac.uk

Key words: Soft Chemical Ionisation-Mass Spectrometry; Proton Transfer Reaction Mass Spectrometry; PTR-MS; phthalate esters; phthalates.

Graphical Abstract

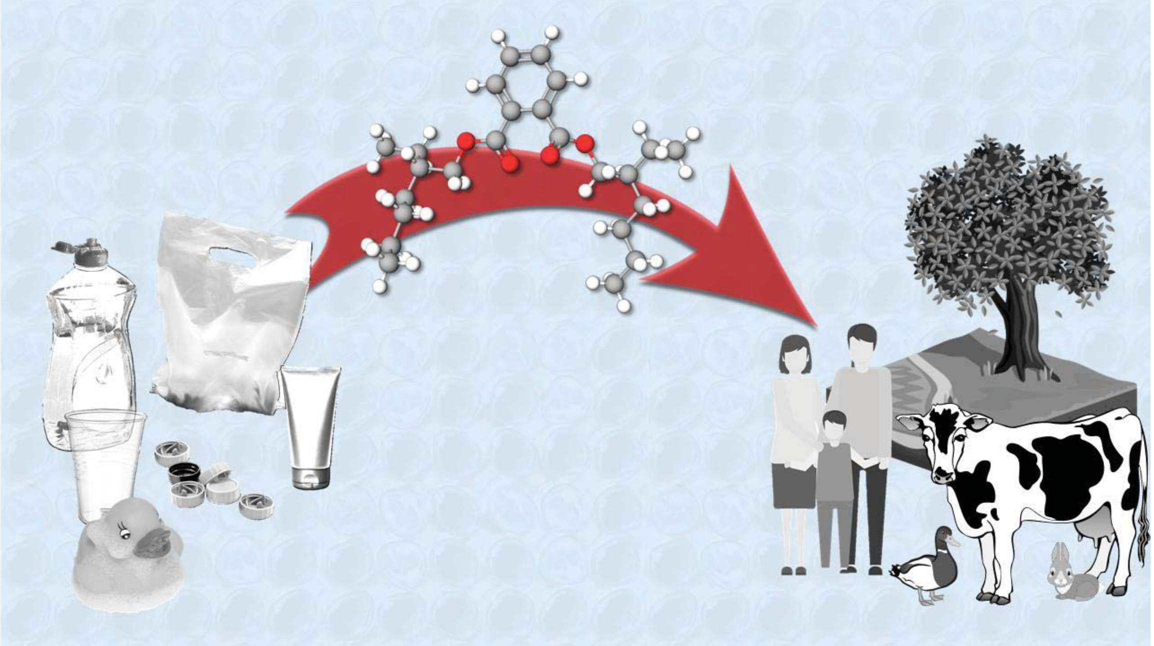

Research highlights

- **First investigations on the use of proton transfer reaction-mass spectrometry for detecting phthalate compounds**
- **Identification of product ion pathways as a function of the reduced electric field**

Abstract

One of the most common environmentally relevant groups of pollutants are phthalate esters. After decades of industrial use, they have become ubiquitous in the environment and analytical methods to chemically detect them in trace amounts are required. In this study, details of Proton Transfer Reaction-Mass Spectrometry (PTR-MS) investigations for the reactions of phthalic acid and ten phthalate esters with H_3O^+ as a function of the reduced electric field are presented. A characteristic product ion observed for several of the phthalate esters is protonated phthalic anhydride (*m/z* 149.02, $C_8H_5O_3^+$). However, not all of the phthalates investigated in this study fragment to produce this product ion following proton transfer. For alkyl diester phthalates, loss of the corresponding alcohol results in the main product ion, but its abundance decreases with increasing alkyl chain length, whilst in comparison for the dialkyl ester phthalates, the protonated phthalic anhydride ion abundance increases with increasing alkyl chain length and with increasing reduced electric field. Collisional induced dissociation in the drift tube of the PTR-MS is shown to be useful as means to manipulate the underlying ion chemistry, leading to unique product ions distinctive to phthalates. The results reported in this work represent a wealth of new data that will be of use for developing a PTR-MS analytical method for the quick, selective and reliable identification of phthalates in the environment.

1. Introduction

Phthalate esters, simply known as phthalates, are the dialkyl, diaryl or alkyl aryl esters of ortho-phthalic acid. Their structure consists of two ester groups attached to two consecutive carbons of a benzene ring (Figure 1), and they form a family of chemicals commonly used as additives in the polymer industry, mainly as plasticisers, since the 1930s.[1] They can be found in a wide range of products, ranging from paints, food packaging, cosmetics, toys, building materials, pharmaceuticals to personal care products.[2,3,4] Hence, they have become ubiquitous xenobiotic pollutants in the environment. [5,6,7]

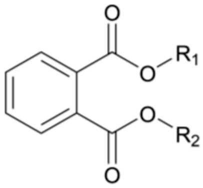

Figure 1: Generic chemical structure of ortho phthalates (R1, R2 groups can be linear, branched, a combination of both or a cyclic ring).

Phthalates are considered to be endocrine disruptors and human carcinogens.[8,9] and have been listed as priority water pollutants. Their use is now either banned or limited by the European Union, United States, China, Canada, and several other countries.[10,11,12,13,14] Thus, human health and environmental concerns arising from decades of phthalates exposure have led to the application of several analytical techniques to the detection and quantification of these plasticisers. Mass spectrometry-based techniques are some of the most commonly used,[15] either with a chromatographic front-end separation,[16,17,18] or without.[19,20,21,22,23] One type of analytical technology that does not commonly use chromatographic separation, and hence can be used in real time is direct injection mass spectrometry (DIMS),[24] of which Proton Transfer Reaction-Mass Spectrometry (PTR-MS) is a commonly used technique.[25]

PTR-MS has found use in a broad range of analytical fields and applications, spanning from environmental analysis, to food science, atmospheric chemistry, health science, and homeland security.[24,25,26,27,28-37] In a previous study by González-Méndez *et al.*, dealing with PTR-MS and smokeless powder, there was an indication of phthalate compounds being present in the powders.[36] In a continuation of that study we present here a novel PTR-MS investigation involving a number of phthalates, namely; phthalic acid (PAcid), dimethyl phthalate (DMP), diethyl phthalate (DEP), diallyl phthalate (DAP), dipropyl phthalate (DPP), dibutyl phthalate (DBP), mono(2-ethylhexyl) phthalate (MEHP), diisobutyl phthalate (DiBP), benzyl butyl phthalate (BBP), dibenzyl phthalate (DBeP) and di(2-ethylhexyl) phthalate (DEHP). To the best of our knowledge, there are no other published PTR-MS studies of phthalates. Therefore, the data presented in this paper addresses this lack of information by providing information on the product ions resulting from their reactions with H_3O^+ as a function of reduced electric field E/N (the ratio of the electric field strength (E) to the gas number density (N)). This informs us as to what product ions should be monitored and at what reduced electric field operational conditions for best sensitivity and selectivity.

2. Experimental Details and methods

2.1. Proton transfer reaction mass spectrometry (PTR-MS)

PTR-MS is a chemical ionisation technique based on ion/molecule reactions between reagent ions, namely $H_3O^+.(H_2O)_n$ (n = 0, 1, 2, and 3) and traces of neutral organic molecules directly injected in the drift tube (DT) of the instrument, whilst an electric field E is applied, and pressure, temperature and humidity are maintained at fixed values. The reagent ions are generated in a glow discharge through a series of ion/molecule processes and transferred to the DT by an applied voltage gradient. As the reagent ions migrate down the DT under the influence of the applied electric field, they may react with neutral trace analyte molecules, resulting in the protonated analyte molecule and/or fragment product ions. The latter results from spontaneous dissociative proton transfer and/or collisional induced dissociation (CID), with CID being enhanced with increasing reduced electric field. A fraction of the reagent and product ions are then transferred to the mass spectrometer for separation and detection.

For the work presented in this paper, a Kore Technology Ltd. Series I Proton Transfer Reaction - Time of Flight-Mass Spectrometer (PTR-ToF-MS) instrument was used, details of which have been given elsewhere. [25,38] Therefore, only brief and pertinent details will be provided in this paper.

Oxygen-free nitrogen (99.998% purity, BOC Gases, Manchester, UK) was used as the carrier gas. The use of a dry buffer gas resulted in H_3O^+ being the dominant reagent ion for the complete range of reduced electric fields, as illustrated in Figure 1. Any contribution from $H_3O^+.(H_2O)_n$ ($n > 0$) to the total reagent ion signal was negligible (3% or less) across the whole E/N range. Thus the reactions with H_3O^+ dominate. Proton transfer from this reagent ion to a compound is facile if the proton affinity (PA) of the analyte is higher than that of water ($PA(H_2O) = 691$ kJ mol^{-1}), although it should be appreciated that sensitive detection of analytes is still possible when this is not the case providing proton transfer is dissociative.[39]

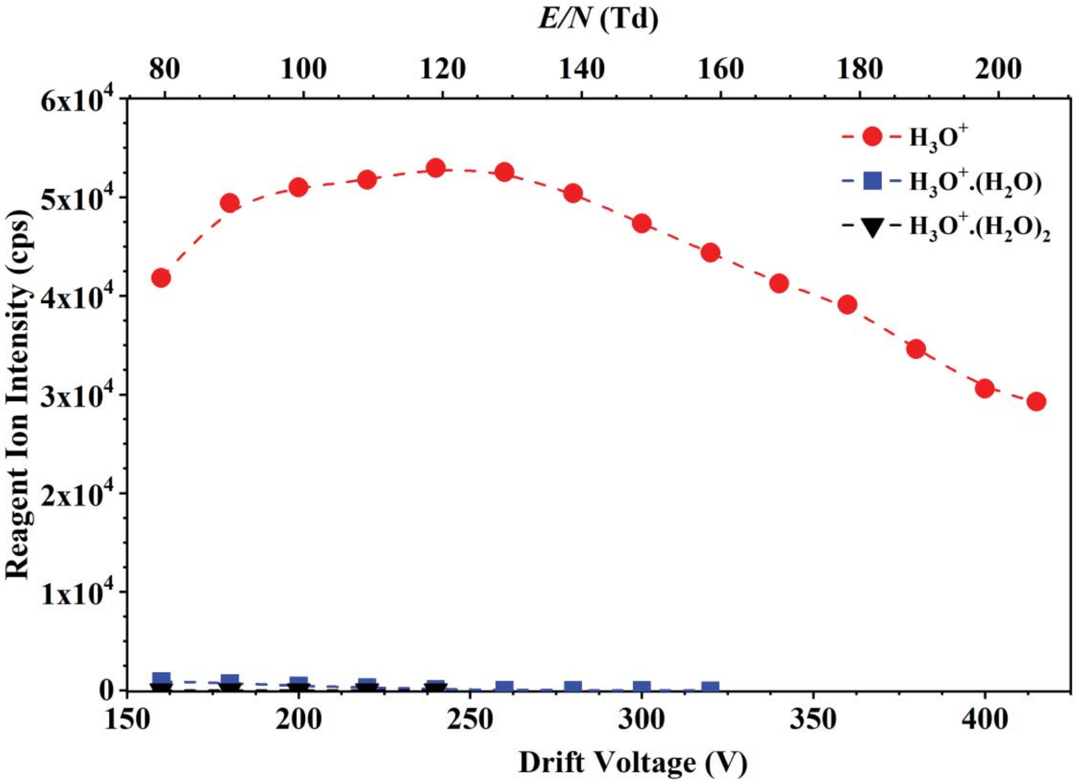

Figure 2. Reagent ion intensities, in counts per second (cps), of $H_3O^+.(H_2O)_n$, $n = 0$, 1, and 2 recorded at the detector of the KORE PTR-ToF-MS as a function of reduced electric field (approximately 80-205 Td).

Water vapour was introduced into the hollow cathode via a mass flow controller to obtain an operating pressure of 1.15 mbar. The drift tube pressure was set to 1.10 mbar. The inlet line and reaction region were both maintained at a temperature of 100 ◦C. To change the reduced electric field value, the operating drift tube voltage was adjusted from 160 V up to 410 V. At the operating pressure used, this provided an *E/N* range of approximately 75- 250 Td.

The headspace above each compound was transferred to the inlet of the PTR-ToF-MS via dynamic headspace using oxygen-free nitrogen (99.998% purity, BOC Gases, Manchester, UK) as carrier gas. The carrier gas was introduced into a glass vial containing typically 2.5 mL of phthalate samples through a septum using a polyether ether ketone (PEEK) capillary. An identical outlet capillary was connected to the inlet system of the PTR-ToF-MS. If no signal was observed at room temperature, the vial was heated to 30 ºC in order to improve signal intensity.

Two mass spectra, with an integration time of 10 seconds, for every phthalate were recorded for each *E/N* value. The averaged mass spectra were then used for analysis.

2.2 Chemicals

Individual samples were purchased from Sigma Aldrich (Cheshire, UK), unless otherwise stated, and used without further purification. These, in order of molecular weight, are PAcid (99.5%), DMP (Acros Organics, Thermo Fisher Scientific, Schwerte, Germany, 99%), DEP (99.5%), DAP (97%), DPP (98%), DBP (99%), MEHP (97%), DiBP (99%), BBP (98%), DEHP (96%) and DBeP (Alfa Aesar, Thermo Fisher Scientific (Kandel) GmbH, Kandel, Germany, 97%). For structural information and other details see Table 1.

Table 1. Compound name, acronym, monoisotopic mass, molecular formula, vapour pressure at 25 °C (in mbar),[40] and chemical structure of the compounds in order of increasing molecular mass.

Compound	**Molecular formula**	**Monoisotopic mass**	**P_{vap} (mbar)**	**Chemical structure**
Phthalic acid, PAcid	$C_8H_6O_4$	166.027	8.48×10^{-7}	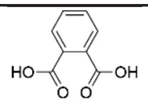
Dimethyl phthalate, DMP	$C_{10}H_{10}O_4$	194.06	4.11×10^{-3}	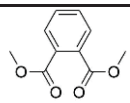
Diethyl phthalate, DEP	$C_{12}H_{14}O_4$	222.09	2.80×10^{-3}	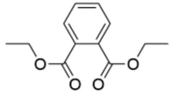
Diallyl phthalate DAP	$C_{14}H_{14}O_4$	246.09	2.68×10^{-4}	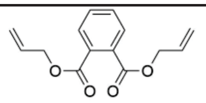
Dipropyl phthalate DPP	$C_{14}H_{18}O_4$	250.12	1.76×10^{-4}	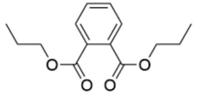
Dibutyl phthalate DBP	$C_{16}H_{22}O_4$	278.15	2.68×10^{-5}	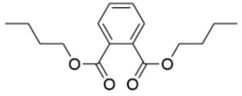
Mono(2-ethylhexyl) phthalate MEHP	$C_{16}H_{22}O_4$	278.15	1.08×10^{-6}	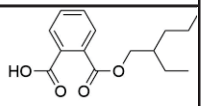
Di-isobutyl phthalate DiBP	$C_{16}H_{22}O_4$	278.15	5.41×10^{-4}	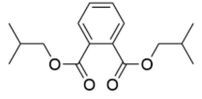
Benzyl butyl phthalate BBP	$C_{19}H_{20}O_4$	312.14	1.10×10^{-5}	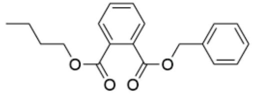

Di(2-ethylhexyl) phthalate DEHP	$C_{24}H_{38}O_4$	390.28	1.89×10^{-7}	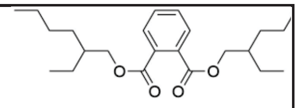
Dibenzyl phthalate DBeP	$C_{22}H_{18}O_4$	458.26	1.59×10^{-6}	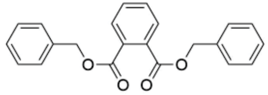

2.3 DFT Calculations

Density functional theory (DFT) calculations have been undertaken to determine the proton affinities (PAs) and gas-phase basicities (GBs) for the compounds of interest. These calculations were conducted using Gaussian09W and GaussView05 for Windows.[41] The B3LYP functional with the 6-31+G(d,p) basis set was used throughout, a combination which has been found to be satisfactory based on our previous work.[42,43]

3. Results and discussion

3.1. DFT calculations

The adjacent carboxyl/esters groups' stereochemistry for most of the compounds of interest means that multiple stable conformations of the protonated species are possible. Whilst they are all accessible given the GBs, interconversion requires group rotation involving transition states. Loss of water or an alcohol can occur from each of these conformations leading to one or the other of the two conformations of protonated phthalic anhydride. For the diethyl ester compounds, more complex calculations are required given that sequential fragmentation occurs. A thorough calculation for these values will be lengthy and involve multiple stable conformations, and that is not within the scope of this work. Given the apparently simple fragmentations of phthalic acid and its dimethyl ester, this presents an interesting chemical question that will be dealt with in a separate paper. However, obtaining approximate PAs and GBs of the studied substances is possible. All the diesters will have very similar PAs and GBs to the dimethyl ester (DMP) and mono(2-ethylhexyl) phthalate (MEHP) – these are 940 and 903 kJ mol^{-1}, and 942 and 903 kJ mol^{-1}, respectively, for their most stable conformation. Phthalic acid itself has a calculated PA of 909 kJ mol^{-1} and GB of 872 kJ mol^{-1} for the most stable conformation. The DFT-calculated PAs and GBs of $(H_2O)_n$ are 684 and 653 kJ mol^{-1}; 842 and 777 kJ mol^{-1}; and 937 and 841 kJ mol^{-1} for $n = 0$, 1 and 2, respectively. Therefore, the compounds investigated in this study can undergo facile proton transfer from $H_3O^+.(H_2O)_n$ ($n = 0, 1, 2$).

3.2. Product ions and their distributions as a function of *E/N*

For this section, only product ions with product ion distribution percentages greater than 3% for any given reduced electric field value are reported. Given that the reagent ion signal is > 97% of H_3O^+ for any given *E/N*, the reaction of H_3O^+ with any given phthalate dominates. The relative product ion abundances reported have an uncertainty of approximately 10%. In all cases, monoisotopic masses have been calculated using the lightest isotopomer. However, when calculating the product ion distributions, we considered all of the isotopologues. For the product ion distribution (PID) plots (given in percentages), the voltage applied to the drift tube is shown in the main *x*-axis, and the reduced electric field *E/N* achieved for that particular voltage is shown on the secondary *x*-axis. Product ions have been tentatively assigned based on the 2 decimal figures exact peak mass and isotopic patterns (^{13}C) intensities.

The most common fragmentation pathway observed is represented in Figure 3. This consists of an α-cleavage of the molecular ion, losing an $-R_1OH$ group, followed by an intramolecular McLafferty rearrangement, dissociating the $-[R_2\text{-}H]$ moiety, to form protonated phthalic anhydride (i.e. *m/z* 149.02).[44] This product ion, however, is not observed for all the phthalates (e.g. it is not detected for dimethyl and diallyl phthalate). Another common product ion is the one arising from the loss of a formate ester group from the protonated parent.

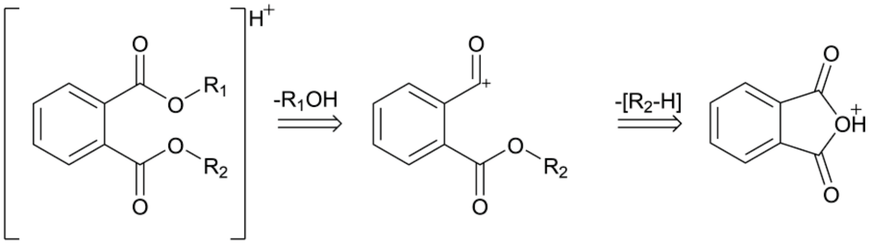

Figure 3: General fragmentation pathway from the protonated parent to protonated phthalic anhydride at *m/z* 149.02. Note that the neutral molecules are omitted.

3.2.1 Phthalic acid (PAcid)

Figure 4 shows the PID plot for the reaction of H_3O^+ with phthalic acid as a function of the reduced electric field. Only two product ions were observed: the protonated parent molecule ($[C_8H_6O_4].H^+$) at *m/z* 167.03 and protonated phthalic anhydride ($C_8H_5O_3^+$) at *m/z* 149.02. The latter is a characteristic phthalate product ion and is observed with many of these compounds.[44]

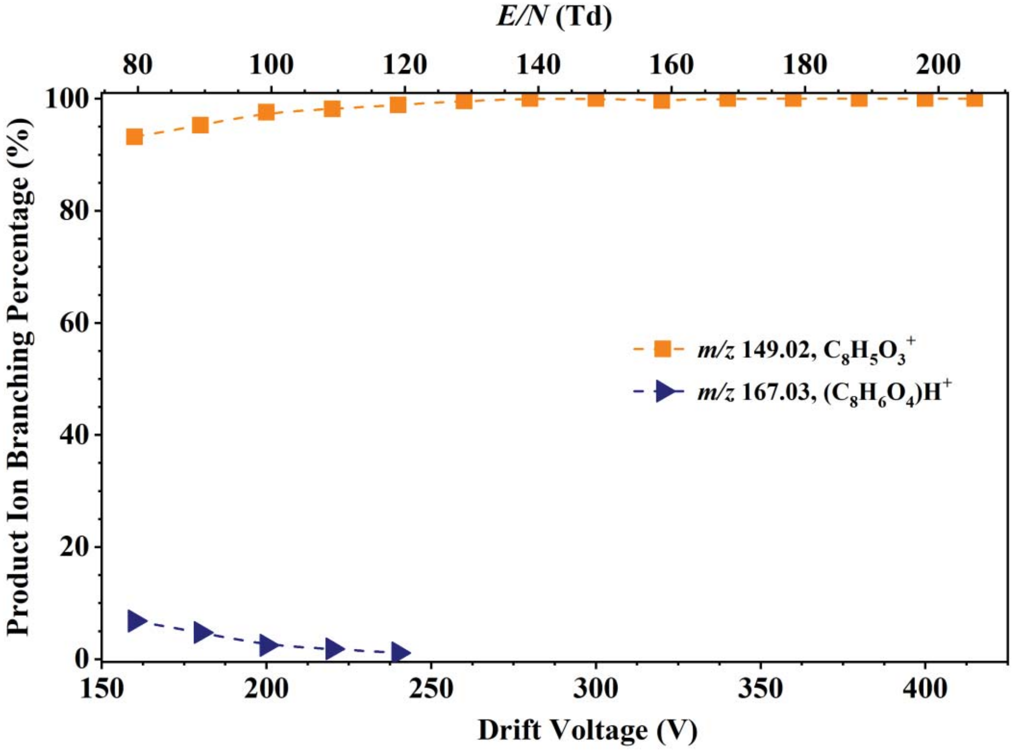

Figure 4: Percentage product ion distribution resulting from the reaction of phthalic acid with H_3O^+ as a function of the drift voltage and the reduced electric field in the range from 80 to 205 Td.

3.2.2 Dimethyl phthalate (DMP)

Dissociative proton transfer to yield $C_9H_7O_3^+$ at *m/z* 163.04, resulting from the loss of methanol from the protonated parent, is the dominant channel for the reaction of DMP with H_3O^+ (Figure 5). The protonated parent ion, $[C_{10}H_{10}O_4].H^+$ at *m/z* 195.07, only represents ca. 25% of the total product ion signal at around 80 Td and its intensity steadily decreases as the *E/N* increases. DMP is the only one of the alkyl diester phthalates studied here in which protonated phthalic anhydride is not a product ion. Protonated phthalic anhydride ion is also observed in GC-MS studies of phthalates.[18, 44]

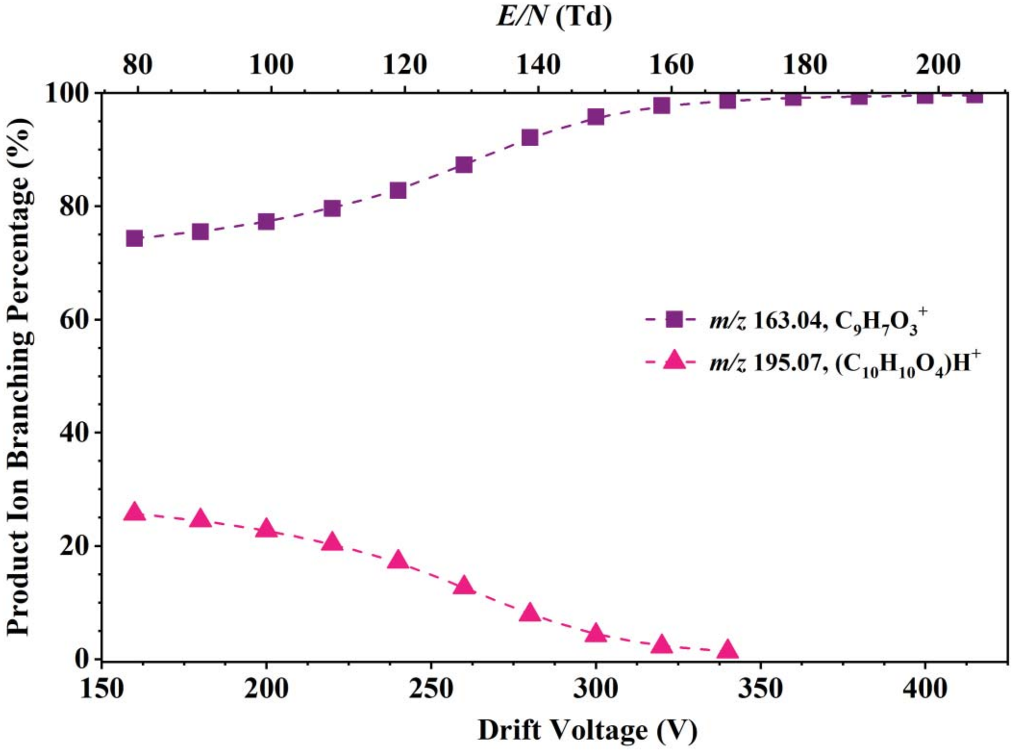

Figure 5: Percentage product ion distribution resulting from the reaction of DMP with H_3O^+ as a function of the drift voltage and the reduced electric field in the range from 80 to 205 Td.

3.2.3 Diethyl phthalate (DEP)

Figure 6 shows the PID plot for the reaction of DEP with H_3O^+ as a function of the drift voltage and the reduced electric field. At low *E/N*, the most abundant ion at ca. 60% is the protonated parent, $[C_{12}H_{14}O_4].H^+$ at *m/z* 223.10. Its intensity steadily decreases as the reduced electric field increases. For *E/N* values below 140 Td, a product ion at *m/z* 75.04 is observed. This is tentatively assigned to protonated ethyl formate ($C_3H_7O_2^+$). The ion at *m/z* 177.05, presumably results from the loss of ethanol from the protonated parent, and hence is assigned to $C_{10}H_9O_3^+$. This product ion peaks at around 150 Td with ca. 65% of the total product ion signal. For *E/N* above 170 Td, the dominant ion is protonated phthalic anhydride ($C_8H_5O_3^+$), formed through collision-induced dissociation, reaching 95% of the total intensity at 210 Td.

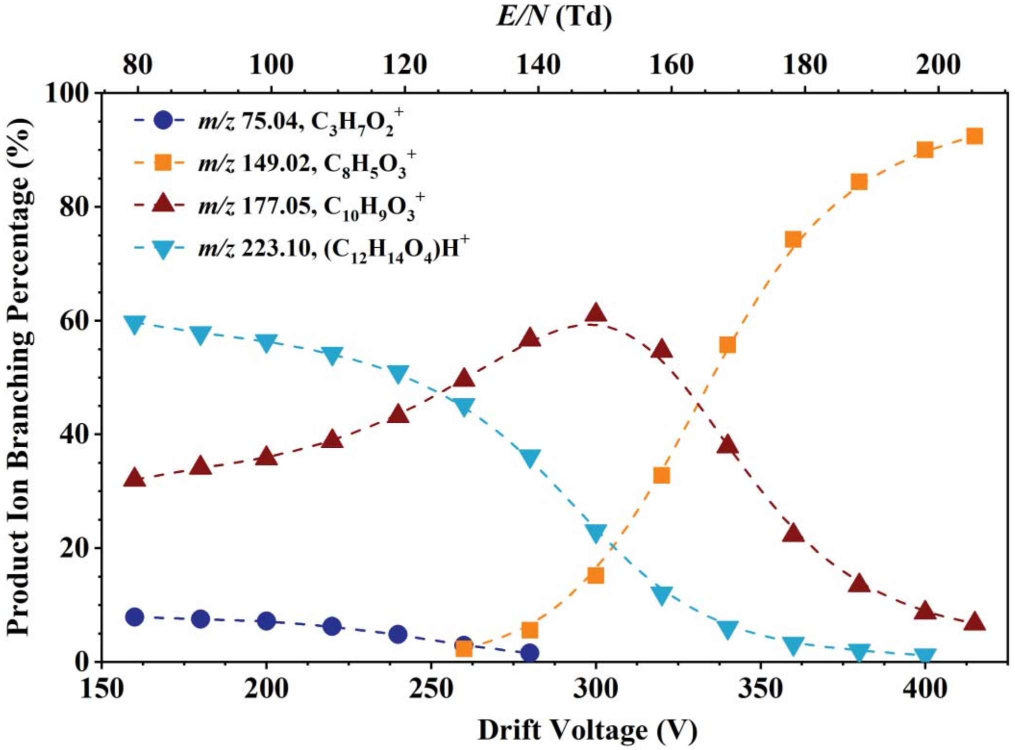

Figure 6: Percentage product ion distribution resulting from the reaction of DEP with H_3O^+ as a function of the drift voltage and the reduced electric field in the range from 80 to 205 Td.

3.2.4 Diallyl phthalate (DAP)

The dominant product ion for the reaction of DAP with H_3O^+ from approximately 80 Td up to around 150 Td (Figure 7), is at *m/z* 247.10, corresponding to the protonated parent, $[C_{14}H_{14}O_4].H^+$ .Above 170 Td product ions $C_{11}H_9O_3^+$ at *m/z* 189.06, resulting from the loss of allyl alcohol, $C_3H_5^+$ at *m/z* 41.04, tentatively assigned to the allyl radical, and $C_3H_3^+$ at *m/z* 39.02 dominate. These ions are produced in a cascade-like fragmentation pathway as the collisional energy increases. Similarly to DMP, protonated phthalic anhydride was not observed in the DAP measurements.

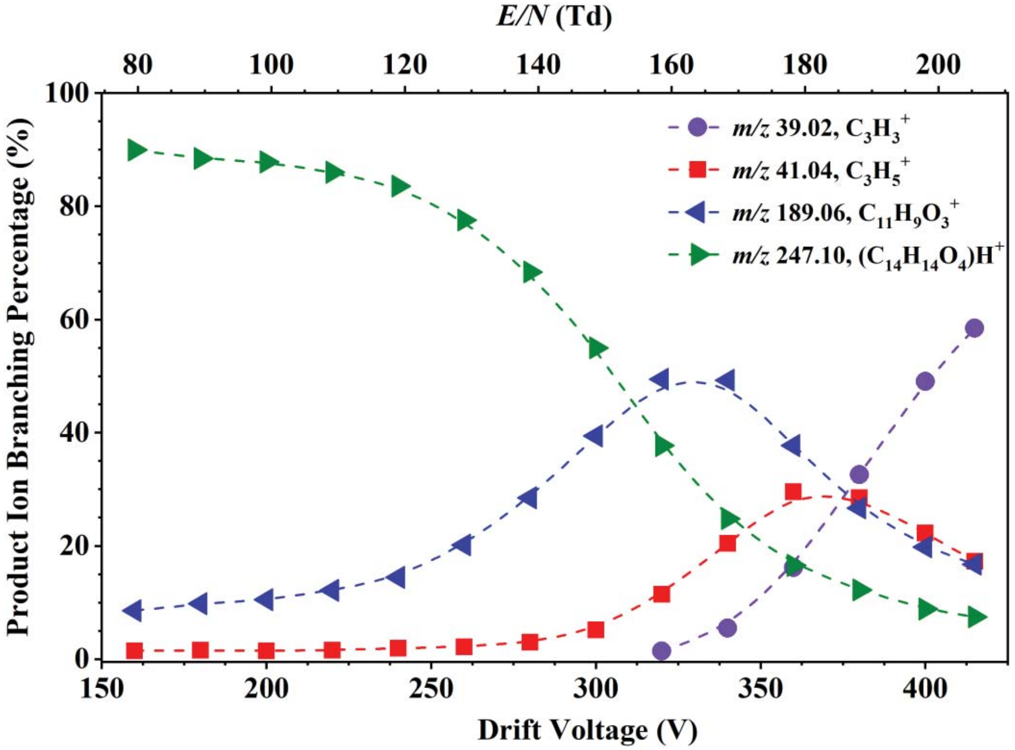

Figure 7: Percentage product ion distribution resulting from the reaction of DAP with H_3O^+ as a function of the drift voltage and the reduced electric field in the range from 80 to 205 Td.

3.2.5 Dipropyl phthalate (DPP)

Figure 8 shows the PID for the reaction of H_3O^+ with DPP as a function of the reduced electric field in the range from 80 to 205 Td. At low *E/N*, the dominant ion is the protonated parent $[C_{14}H_{18}O_4].H^+$ at *m/z* 251.13, followed by the loss of one of the propyl formate (i.e. $C_4H_6O_2$) branches from the protonated parent, yielding $C_{10}H_{13}O_2^+$, tentatively assigned to protonated propyl benzoate, and the loss of propanol from the protonated parent, yielding $C_{11}H_{11}O_3^+$. The abundance of these three ions decrease with increasing reduced electric field and at ca. 150 Td protonated phthalic anhydride *m/z* 149.02 becomes dominant. The ions found at high *E/N* are protonated benzoic acid ($C_7H_7O_2^+$, *m/z* 123.04) and protonated benzene ($C_6H_7^+$, *m/z* 79.05). A minor contribution is observed for the whole *E/N* range from charged benzoyl ion ($C_7H_5O^+$, *m/z* 105.03).

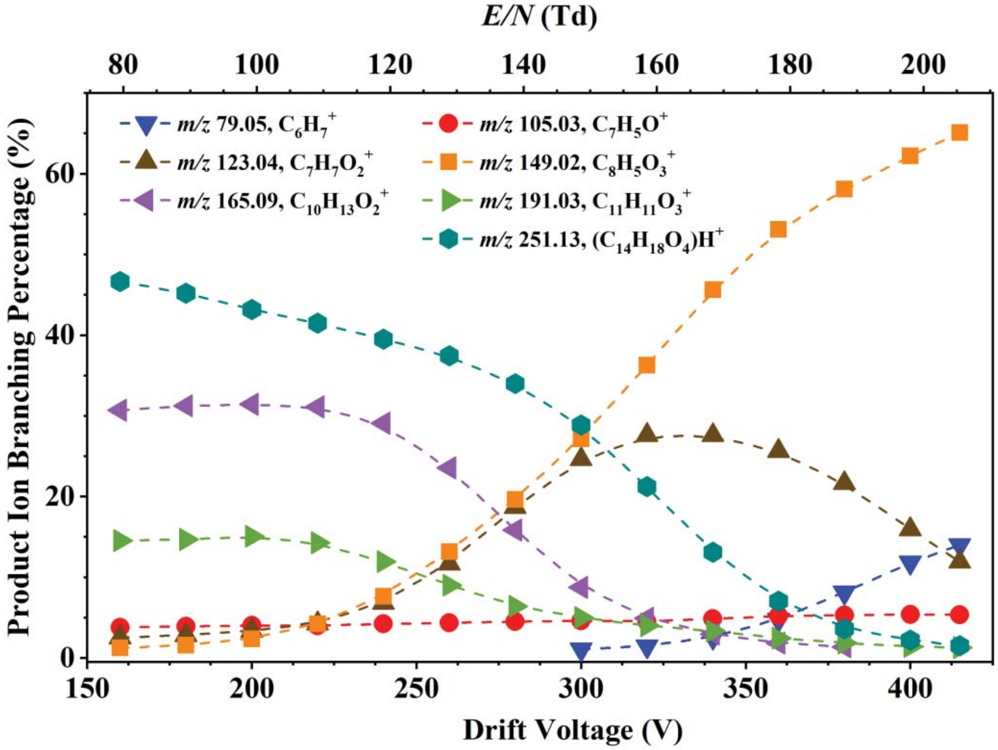

Figure 8: Percentage product ion distribution resulting from the reaction of DPP with H_3O^+ as a function of the drift voltage and the reduced electric field in the range from 80 to 205 Td.

3.2.6 Dibutyl phthalate (DBP)

The protonated parent ion $[C_{16}H_{22}O_4].H^+$ at *m/z* 279.16 is the most abundant ion from low *E/N* up to around 130 Td, after which protonated phthalic anhydride becomes the most abundant ion for the rest of the reduced electric field range (see Figure 9). At low *E/N* we also observed an ion resulting from the loss of butanol from the protonated parent, $C_{12}H_{13}O_3^+$ at *m/z* 205.09, and another ion caused by the loss of butyl formate (i.e. $C_5H_8O_2$) to yield $C_{11}H_{15}O_2^+$ at *m/z* 179.10, which is tentatively assigned to protonated butyl benzoate. At high *E/N* some minor ions are protonated benzoic acid ($C_7H_7O_2^+$), charged benzoyl ($C_7H_5O^+$) and protonated benzene ($C_6H_7^+$) at *m/z* 123.04, *m/z* 105.03 and *m/z* 79.05, respectively.

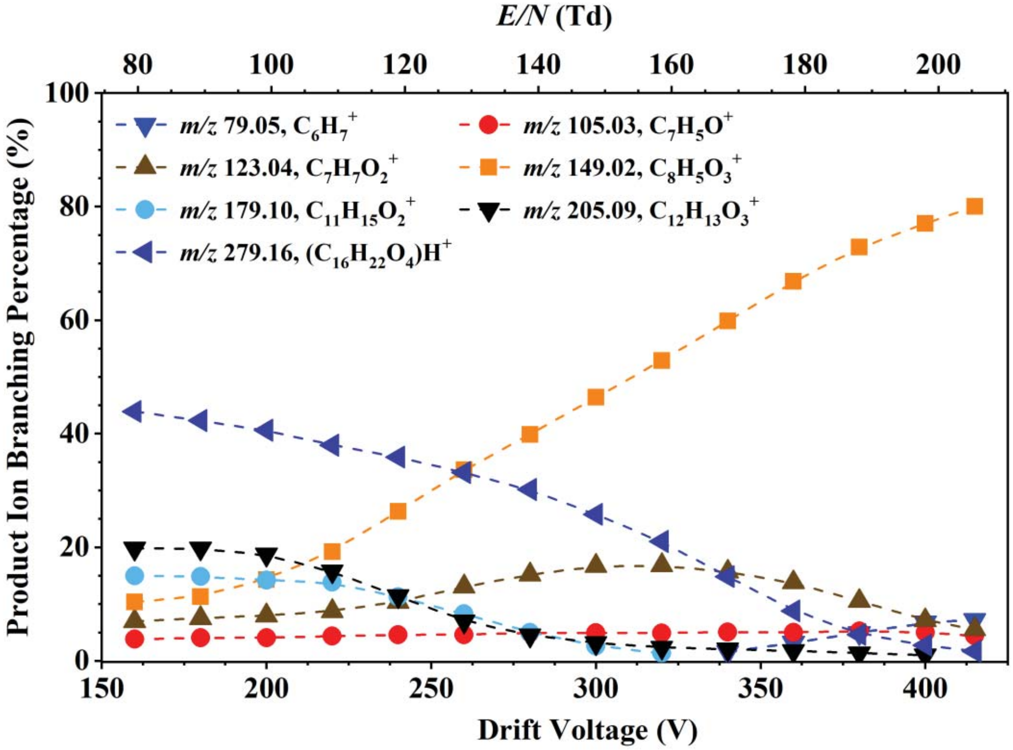

Figure 9: Percentage product ion distribution resulting from the reaction of DBP with H_3O^+ as a function of the drift voltage and the reduced electric field in the range from 80 to 205 Td.

3.2.7 Monoethylhexyl phthalate (MEHP)

Protonated phthalic anhydride is the dominant product ion for all the *E/N* range for the reaction of MEHP with H_3O^+ (Figure 10). The protonated parent (i.e. *m/z* 279.16) was not observed for any reduced electric field value. Another ion, $C_8H_{17}O^+$, at *m/z* 129.13, is tentatively assigned to protonated 2-ethylhexanal. The other observed product ions, $C_8H_{17}^+$ at *m/z* 113.13, $C_8H_{15}^+$ at *m/z* 111.12, $C_5H_{11}^+$ at *m/z* 71.09, $C_5H_9^+$ at *m/z* 69.07, $C_4H_9^+$ at *m/z* 57.07, $C_3H_7^+$ at *m/z* 43.05, $C_3H_5^+$ at *m/z* 41.04 and $C_3H_3^+$ at *m/z* 39.02, potentially come from successive fragmentation of protonated 2-ethylhexanal.

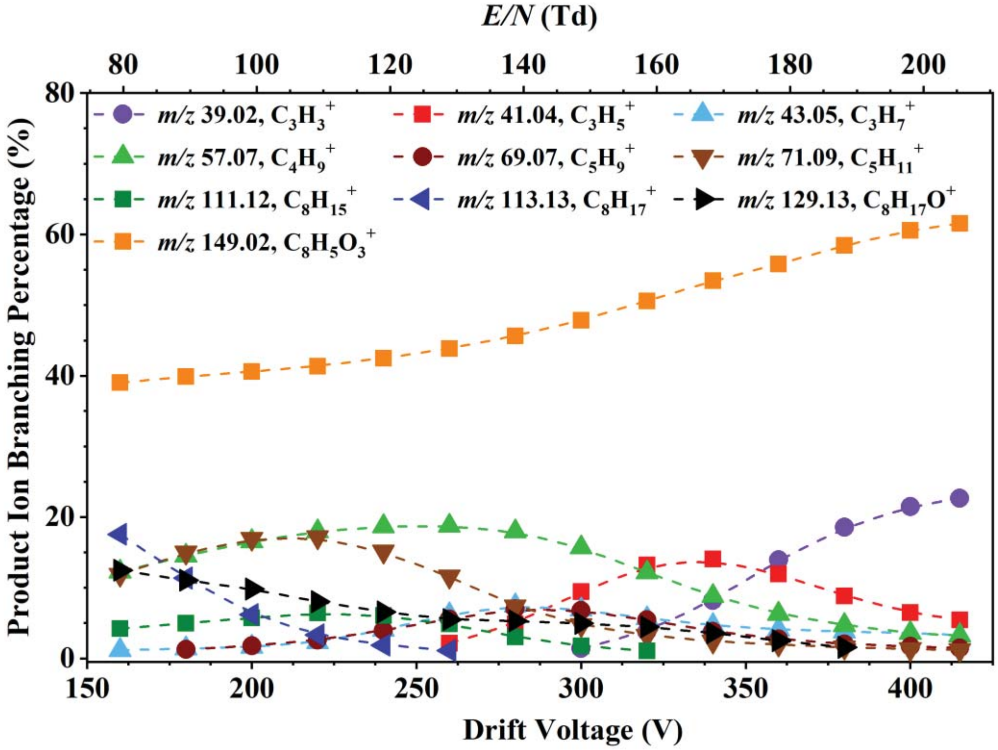

Figure 10: Percentage product ion distribution resulting from the reaction of MEHP with H_3O^+ as a function of the drift voltage and the reduced electric field in the range from 80 to 205 Td.

3.2.8 Diisobutyl phthalate (DiBP)

The PID of the reaction of DiBP with H_3O^+ (Figure 11) is similar to that of its isomer DBP (Figure 9), observing the same product ions, but with different relative percentages. The two dominant ions are the protonated parent ($[C_{16}H_{22}O_4].H^+$ at *m/z* 279.16) predominantly observed at lower *E/N* and protonated phthalic anhydride at higher *E/N*. For DiBP the crossover point is at ca. 170 Td, instead of at ca. 130 Td for DBP. At low *E/N* there are traces of the loss of isobutanol from the protonated parent molecule ($C_{12}H_{13}O_3^+$ at *m/z* 205.09).

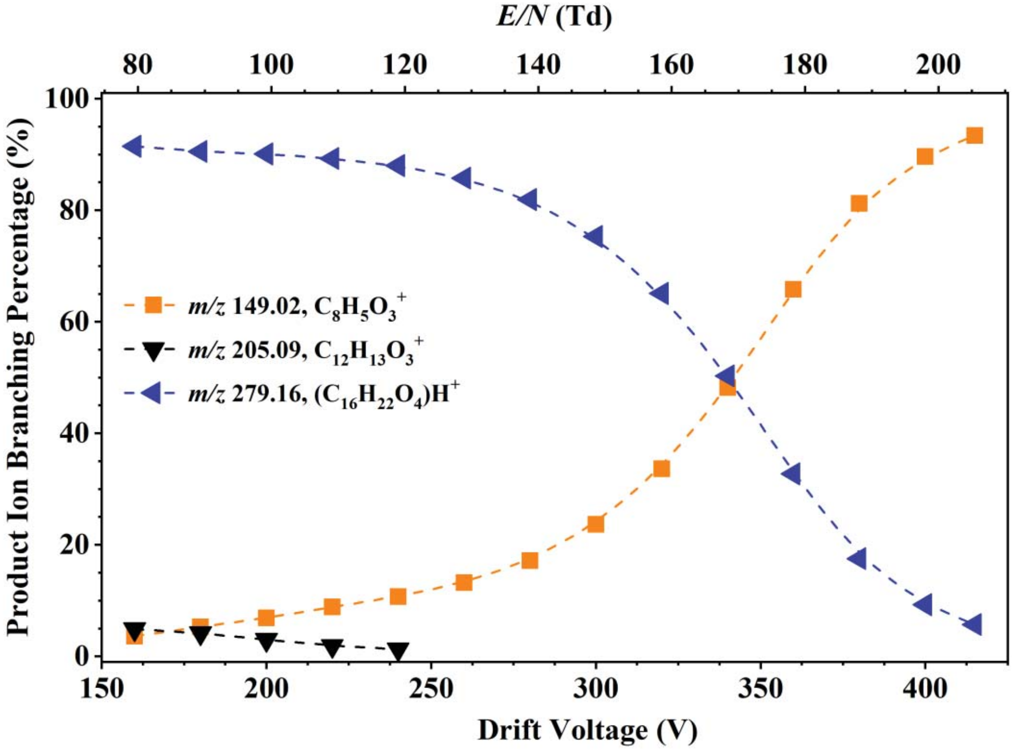

Figure 11: Percentage product ion distribution resulting from the reaction of DiBP with H_3O^+ as a function of the drift voltage and the reduced electric field in the range from 80 to 205 Td.

3.2.9 Benzyl butyl phthalate and dibenzyl phthalate (BBP and DBeP)

BBP and DBeP have a benzyl ester group in common and this seems to be crucial in the proton transfer and fragmentation processes as they show very similar product ion distributions (Figure 12). The product ion at *m/z* 91.05, assigned to be $C_7H_7^+$, dominates throughout the whole *E/N* range. The identity of this ion is supposedly assigned to be the tropylium ion, formed from the rearrangement of the benzyl cation ($C_6H_5CH_2^+$) to a more energetically stable cyclic aromatic structure.[45] This ion is commonly observed in compounds containing a benzyl group.[46] Two other product ions are observed for both BBP and DBeP with a lower branching percentage than $C_7H_7^+$, these are $C_7H_7O^+$, *m/z* 107.05, tentatively assigned to protonated benzaldehyde, and $C_6H_7^+$, *m/z* 79.05, which is tentatively assigned to protonated benzene.

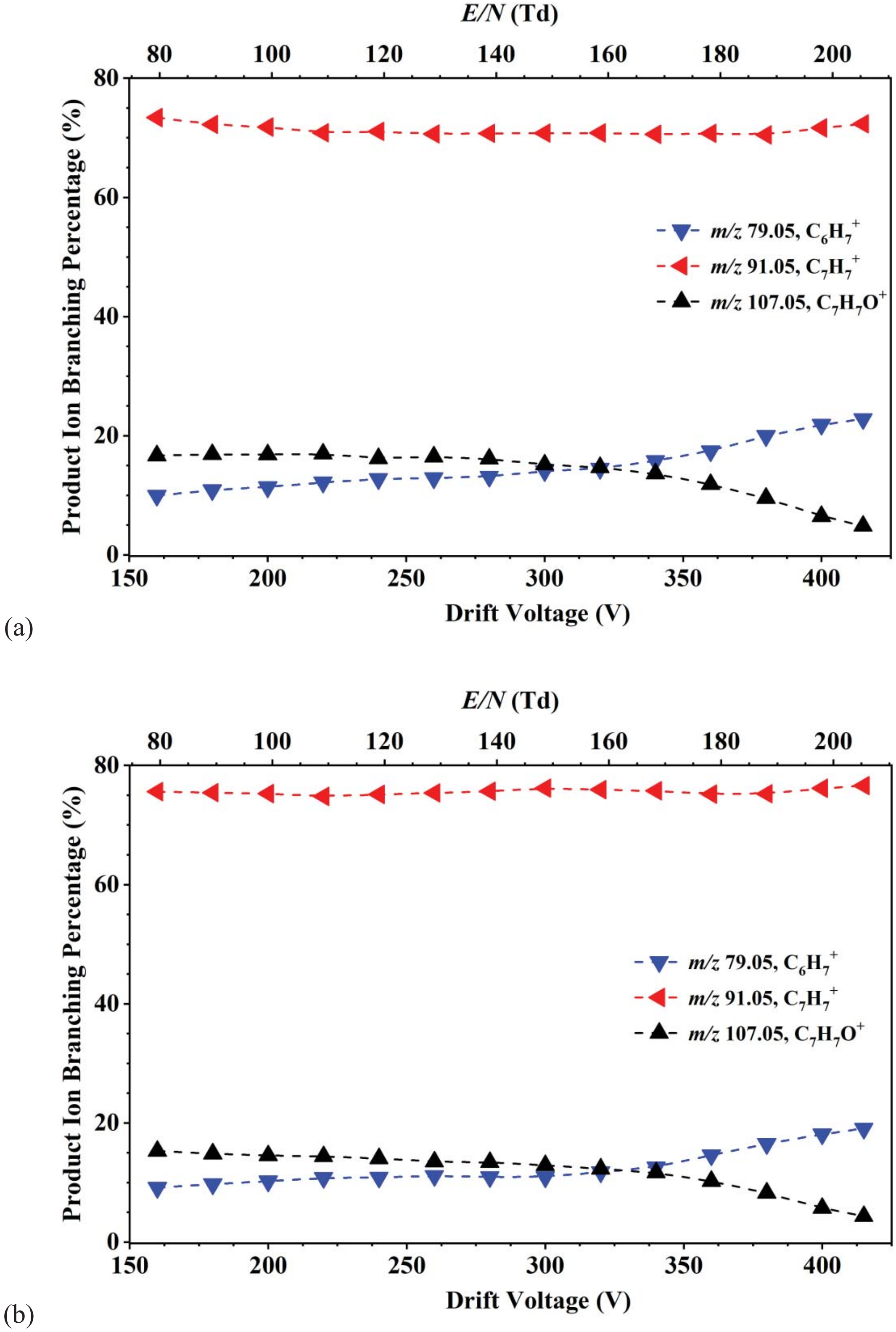

Figure 12: Percentage product ion distribution resulting from the reaction of (a) BBP and (b) DBeP with H_3O^+ as a function of the drift voltage and the reduced electric field in the range from 80 to 205 Td.

3.2.10 Bis(2-ethylhexyl) phthalate (DEHP)

Figure 13 shows that the reaction of DEHP with H_3O^+ yields a similar PID to that of MEHP (Figure 10). For example, the protonated parent, here $[C_{24}H_{38}O_4].H^+$ at *m/z* 391.40, is not observed. The main difference between MEHP and DEHP is that protonated phthalic anhydride is not the dominant ion for any *E/N* value for DEHP, whilst it is for MEHP. Instead, for DEHP, there are several product ions that become dominant across the studied *E/N* range. Furthermore, the only two product ions observed with DEHP that were not found with MEHP are at *m/z* 235.17, assigned to $C_{15}H_{23}O_2^+$, and *m/z* 123.04, $C_7H_7O_2^+$, tentatively assigned to loss of 2-ethylhexyl formate from the protonated parent and protonated benzoic acid, respectively.

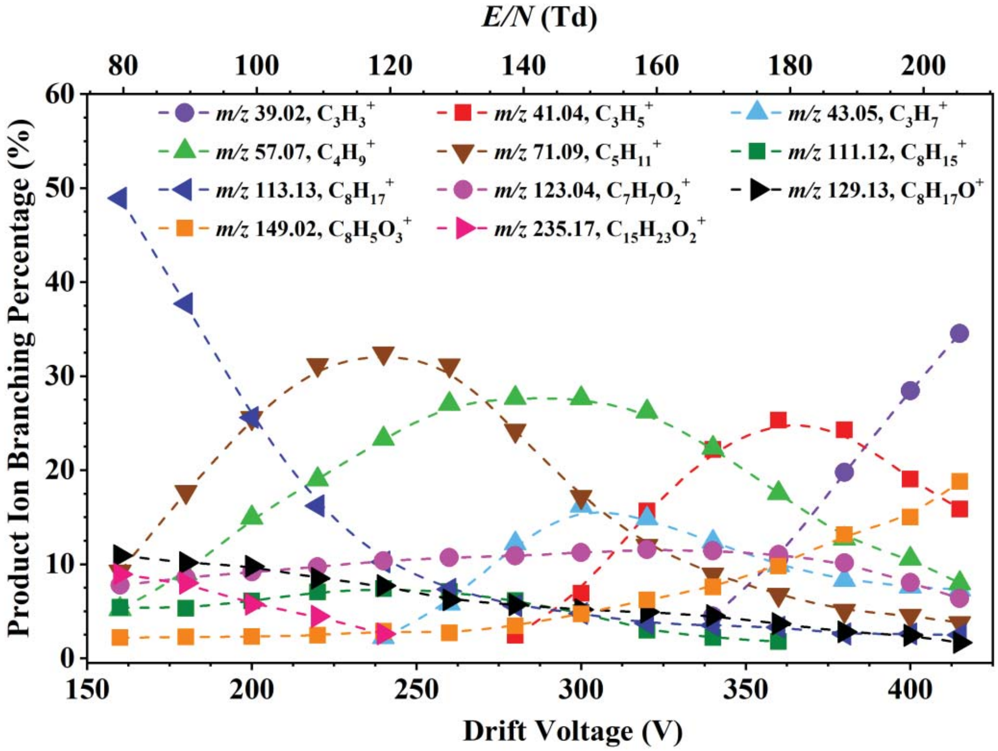

Figure 13: Percentage product ion distribution resulting from the reaction of DEHP with H_3O^+ as a function of the drift voltage and the reduced electric field in the range from 80 to 205 Td.

3.2.11 Separation of isomers: DBP vs DiBP vs MEHP

DBP, DiBP and MEHP are isomers, and thus the protonated parent for these molecules is at the identical *m/z* value ($[C_{16}H_{22}O_4].H^+$, *m/z* 279.16). However, their reaction with H_3O^+ yields different product ions distributions at different reduced electric fields, hence providing a quick and easy method to differentiate between them without the need for pre-separation. The difference between butyl-containing isomers (i.e. DBP and DiBP) and MEHP is the presence of the protonated parent ion at low *E/N* for DBP and DiBP, which is not observed for MEHP.

To distinguish between DBP and DiBP it is necessary to compare other product ions. The main differences between these two isomers is the higher signal of $C_{12}H_{13}O_3^+$ (*m/z* 205.09) from DBP at low *E/N* (i.e. around 20%) and $C_7H_7O_2^+$ (*m/z* 123.04) at high *E/N*. For DiBP, the presence of the former is very little (only ca. 5%) and the latter is less than 3% (and for this reason it is not included in the plots).

4. Conclusions

This study provides the first PTR-MS results of phthalic acid and ten of its ester derivatives. A characteristic product ion observed for many of the phthalates is protonated phthalic anhydride (*m/z* 149.02, $C_8H_5O_3^+$), which is not a surprise as this ion has been widely reported as a phthalate indicator with different mass spectrometric techniques. However, phthalates do not always fragment to produce this ion following proton transfer. For the dialkylester phthalates, the abundance of protonated phthalic anhydride increases with increasing alkyl chain length and with the reduced electric field. Furthermore, protonated phthalic anhydride is the only dominant product ion for reduced electric field values higher than approximately 130 Td for DBP, while for DEHP it only reaches 20% of the total ion signal and for BBP it is not a product ion. Therefore, some caution must be taken before discarding the presence of phthalate esters when *m/z* 149.02 is not a product ion observed in the PTR-MS.

All of the alkyl diester phthalates investigated lose the corresponding alcohol (i.e. methanol for DMP, ethanol for DEP, propanol for DPP and butanol for DBP). The abundance of product ions resulting from the loss of an alcohol decreases with the increasing alkyl chain length. For example, for DMP the loss of methanol (*m/z* 163) results in the dominant ion throughout all of the *E/N* range, while for DBP the loss of butanol results in a product ion at *m/z* 205 that is only ca. 20% at 80 Td, and it steadily decreases with increasing reduced electric field. Protonated benzoate esters are also product ions observed with phthalates after losing a formate group (e.g. propyl benzoate for DPP, butyl benzoate for DBP and 2-ethylhexyl benzoate for DEHP).

Different product ion distributions were found for DBP, DiBP and MEHP, which provides a means to analytically distinguish these three phthalate ester isomers. The range of collisional energies provided by a PTR-MS instrument can therefore be used to manipulate the ion-molecule reactions to yield characteristic and distinguishable fragmentation pathways for improved selectivity. Many of the fragmentation channels were only observed at an *E/N* higher than a certain value, which indicates that they result from field-activated collision-induced dissociation.

We have shown that PTR-MS can analyse the environmentally relevant phthalate compounds. It is worth highlighting that for analysing many samples for phthalates with PTR-MS the adoption of an automated sampling system, as devised for food studies,[47] would be advantageous and considerably enhance the use of PTR-MS.

5. Acknowledgements

We thank the Marie Skłodowska-Curie Actions Innovative Training Network: Ion-Molecule Processes for Analytical Chemistry Technologies (IMPACT) (www.impact-h2020itn.com) which has supported this research through the European Commission's HORIZON 2020 Programme under Grant Agreement Number 674911. DOL is an Early Stage Researcher on IMPACT. The authors wish to thank Dr Peter Watts (member of the Molecular Physics Group, School of Physics and Astronomy, University of Birmingham, UK) for undertaking the DFT calculations presented in this paper.

6. References

1. Booth, G., Ullmann's encyclopedia of industrial chemistry. *Reference Services Review* **2007,** *16* (4), 31-34.
2. Rivera-Utrilla, J.; Ocampo-Pérez, R.; Méndez-Díaz, J. D.; Sánchez-Polo, M., Environmental impact of phthalic acid esters and their removal from water and sediments by different technologies–a review. *Journal of environmental management* **2012,** *109*, 164-178.
3. Staples, C. A.; Peterson, D. R.; Parkerton, T. F.; Adams, W. J., The environmental fate of phthalate esters: a literature review. *Chemosphere* **1997,** *35* (4), 667-749.
4. Fromme, H.; Küchler, T.; Otto, T.; Pilz, K.; Müller, J.; Wenzel, A., Occurrence of phthalates and bisphenol A and F in the environment. *Water research* **2002,** *36* (6), 1429-1438.
5. Liang, D.-W.; Zhang, T.; Fang, H. H.; He, J., Phthalates biodegradation in the environment. *Applied microbiology and Biotechnology* **2008,** *80* (2), 183.
6. Olujimi, O.; Fatoki, O.; Odendaal, J.; Okonkwo, J., Endocrine disrupting chemicals (phenol and phthalates) in the South African environment: a need for more monitoring. *Water SA* **2010,** *36* (5).
7. Gao, D.-W.; Wen, Z.-D., Phthalate esters in the environment: A critical review of their occurrence, biodegradation, and removal during wastewater treatment processes. *Science of the total Environment* **2016,** *541*, 986-1001.
8. Rusyn, I.; Corton, J. C., Mechanistic considerations for human relevance of cancer hazard of di (2-ethylhexyl) phthalate. *Mutation Research/Reviews in Mutation Research* **2012,** *750* (2), 141-158.
9. Wormuth, M.; Scheringer, M.; Vollenweider, M.; Hungerbühler, K., What are the sources of exposure to eight frequently used phthalic acid esters in Europeans? *Risk Analysis* **2006,** *26* (3), 803-824.
10. European Parliament. Directive 2005/84/EC Of The European Parliament And The Council. Official Journal of the European Union 344, 40–43 (2005).
11. European Parliament. European Regulation No 1272/2008 of the European Parliament and of the Council. Official Journal of the European Union 20, 1–1355 (2008).

12. Congress of the United States. Consumer Product Safety Improvement Act (CPSIA) of 2008. Public Law 110–314 (2008).

13. Standardization Administration of the People's Republic of China. GB 6675-2014 Toy Safety Standard Updates. Chinese Standard Publishing House, Beijing (2014).

14. Shaul, J. C.; Trebilcock, M. J., The Administration of the Federal Hazardous Products Act. In *Can. Bus. LJ*, 1982; Vol. 7, p 2.

15. Net, S.; Delmont, A.; Sempéré, R.; Paluselli, A.; Ouddane, B., Reliable quantification of phthalates in environmental matrices (air, water, sludge, sediment and soil): a review. *Science of the Total Environment* **2015,** *515*, 162-180.

16. Fan, J.-c.; Wu, L.; Wang, X.-f.; Huang, X.-h.; Jin, Q.; Wang, S.-t., Determination of the migration of 20 phthalate esters in fatty food packaged with different materials by solid-phase extraction and UHPLC–MS/MS. *Analytical Methods* **2012,** *4* (12), 4168-4175.

17. Blair, J. D.; Ikonomou, M. G.; Kelly, B. C.; Surridge, B.; Gobas, F. A., Ultra-trace determination of phthalate ester metabolites in seawater, sediments, and biota from an urbanized marine inlet by LC/ESI-MS/MS. *Environmental science & technology* **2009,** *43* (16), 6262-6268.

18. Bergh, C.; Torgrip, R.; Östman, C., Simultaneous selective detection of organophosphate and phthalate esters using gas chromatography with positive ion chemical ionization tandem mass spectrometry and its application to indoor air and dust. *Rapid Communications in Mass Spectrometry* **2010,** *24* (19), 2859-2867.

19. Antal, B.; Kuki, Á.; Nagy, L.; Nagy, T.; Zsuga, M.; Kéki, S., Rapid detection of hazardous chemicals in textiles by direct analysis in real-time mass spectrometry (DART-MS). *Analytical and bioanalytical chemistry* **2016,** *408* (19), 5189-5198.

20. Crawford, E.; Crone, C.; Horner, J.; Musselman, B., Food packaging: strategies for rapid phthalate screening in real time by ambient ionization tandem mass spectrometry. In *Chemistry of Food, Food Supplements, and Food Contact Materials: From Production to Plate*, ACS Publications: 2014; pp 71-85.

21. Ohgaki, M.; Takeguchi, Y.; Okawa, S.; Namiki, K., Screening analysis of RoHS directive hazardous substances (phthalate esters and bromodiphenyl ethers) by novel mass spectrometry using soft ionization. *Royal Society open science* **2019,** *6* (2), 181469.

22. Michalczuk, B.; Moravský, L.; Papp, P.; Mach, P.; Sabo, M.; Matejčík, Š., Isomer and conformer selective atmospheric pressure chemical ionisation of dimethyl phthalate. *Physical Chemistry Chemical Physics* **2019,** *21* (25), 13679-13685.

23. Lacko, M.; Michalczuk, B.; Matejčík, Š.; Španěl, P. J. P. C. C. P., Ion chemistry of phthalates in selected ion flow tube mass spectrometry: isomeric effects and secondary reactions with water vapour. **2020,** *22* (28), 16345-16352.

24. Biasioli, F.; Yeretzian, C.; Märk, T. D.; Dewulf, J.; Van Langenhove, H., Direct-injection mass spectrometry adds the time dimension to (B)VOC analysis. *TrAC Trends in Analytical Chemistry* **2011,** *30* (7), 1003-1017.

25. Andrew M. Ellis, C. A. M., *Proton Transfer Reaction Mass Spectrometry: Principles and Applications*. 1^{st} ed.; Wiley: 2014; p 336.

26. Sulzer, P.; Petersson, F.; Agarwal, B.; Becker, K. H.; Jürschik, S.; Märk, T. D.; Perry, D.; Watts, P.; Mayhew, C. A., Proton Transfer Reaction Mass Spectrometry and the Unambiguous Real-Time Detection of 2,4,6 Trinitrotoluene. *Analytical Chemistry* **2012,** *84* (9), 4161-4166.

27. Malásková, M.; Olivenza-León, D.; Piel, F.; Mochalski, P.; Sulzer, P.; Jürschik, S.; Mayhew, C. A.; Märk, T. D. J. R. D. I. I., Radicals, Neutral; Species, E., Compendium H Relevance 3O+ With to Selected Breath of the Reactions Ketones Analysis of of Using Proton Transfer Reaction Mass Spectrometry. **2020**.

28. Sulzer, P.; Agarwal, B.; Jürschik, S.; Lanza, M.; Jordan, A.; Hartungen, E.; Hanel, G.; Märk, L.; Märk, T. D.; González-Méndez, R.; Watts, P.; Mayhew, C. A., Applications of switching reagent ions in proton transfer reaction mass spectrometric instruments for the improved selectivity of explosive compounds. *International Journal of Mass Spectrometry* **2013,** *354–355* (0), 123-128.

29. Agarwal, B.; González-Méndez, R.; Lanza, M.; Sulzer, P.; Märk, T. D.; Thomas, N.; Mayhew, C. A., Sensitivity and Selectivity of Switchable Reagent Ion Soft Chemical Ionization Mass Spectrometry for the Detection of Picric Acid. *The Journal of Physical Chemistry A* **2014,** *118* (37), 8229-8236.

30. González-Méndez, R.; Reich, D. F.; Mullock, S. J.; Corlett, C. A.; Mayhew, C. A., Development and use of a thermal desorption unit and proton transfer reaction mass spectrometry for trace explosive detection: Determination of the instrumental limits of detection and an investigation of memory effects. *International Journal of Mass Spectrometry* **2015,** *385*, 13-18.

31. González-Méndez, R.; Watts, P.; Olivenza-León, D.; Reich, D. F.; Mullock, S. J.; Corlett, C. A.; Cairns, S.; Hickey, P.; Brookes, M.; Mayhew, C. A., Enhancement of Compound Selectivity Using a Radio Frequency Ion-Funnel Proton Transfer Reaction Mass Spectrometer: Improved Specificity for Explosive Compounds. *Analytical Chemistry* **2016,** *88* (21), 10624-10630.

32. Mateirć, D.; Blenkhorn, D.; González-Méndez, R.; Bruhn, D.; Turner, C.; Morgan, G.; Mason, N.; Gauci, V., Monoterpene emission from young scots pine may be influenced by nutrient availability. *Applied Ecology and Environmental Research* **2016,** *14* (4), 667-681.

33. González-Méndez, R. Development and applications of Proton Transfer Reaction-Mass Spectrometry for Homeland Security: trace detection of explosives. PhD, University of Birmingham, 2017.

34. Lourenço, C.; González-Méndez, R.; Reich, F.; Mason, N.; Turner, C., A potential method for comparing instrumental analysis of volatile organic compounds using standards calibrated for the gas phase. *International Journal of Mass Spectrometry* **2017,** *419*, 1-10.

35. González-Méndez, R.; Watts, P.; Reich, D. F.; Mullock, S. J.; Cairns, S.; Hickey, P.; Brookes, M.; Mayhew, C. A., Use of Rapid Reduced Electric Field Switching to Enhance Compound Specificity for Proton Transfer Reaction-Mass Spectrometry. *Analytical Chemistry* **2018,** *90* (9), 5664-5670.

36. González-Méndez, R.; Mayhew, C. A., Applications of Direct Injection Soft Chemical Ionisation-Mass Spectrometry for the Detection of Pre-blast Smokeless Powder Organic Additives. *Journal of The American Society for Mass Spectrometry* **2019,** *30* (4), 615-624.

37. Olivenza-León, D.; Mayhew, C. A.; González-Méndez, R., Selective Reagent Ion Mass Spectrometric Investigations of the Nitroanilines. *Journal of The American Society for Mass Spectrometry* **2019,** *30* (11), 2259-2266.

38. Blake, R. S.; Monks, P. S.; Ellis, A. M., Proton-Transfer Reaction Mass Spectrometry. *Chemical Reviews* **2009,** *109* (3), 861-896.

39. Malásková, M.; Olivenza-León, D.; Chellayah, P. D.; Martini, J.; Lederer, W.; Ruzsanyi, V.; Unterkofler, K.; Mochalski, P.; Märk, T. D.; Watts, P.; Mayhew, C. A., Studies pertaining to the monitoring of volatile halogenated anaesthetics in breath by proton transfer reaction mass spectrometry. *Journal of breath research* **2020,** *14* (2), 026004.

40. (EPA), U. E. P. A. Chemistry Dashboard. https://comptox.epa.gov/dashboard (accessed April 2020).

41. Frisch, M.; Trucks, G.; Schlegel, H.; Scuseria, G.; Robb, M.; Cheeseman, J.; Scalmani, G.; Barone, V.; Mennucci, B.; Petersson, G., Gaussian 09, revision A. 1. *Gaussian Inc., Wallingford, CT* **2009**.

42. González-Méndez, R.; Watts, P.; Howse, D. C.; Procino, I.; McIntyre, H.; Mayhew, C. A., Ion Mobility Studies on the Negative Ion-Molecule Chemistry of Isoflurane and Enflurane. *Journal of The American Society for Mass Spectrometry* **2017,** *28* (5), 939-946.
43. González-Méndez, R.; Watts, P.; Howse, D. C.; Procino, I.; McIntyre, H.; Mayhew, C. A., Ion mobility studies on the negative ion-molecule chemistry of pentachloroethane. *International Journal of Mass Spectrometry* **2017,** *417*, 16-21.
44. Yin, P.; Chen, H.; Liu, X.; Wang, Q.; Jiang, Y.; Pan, R. J. A. L., Mass spectral fragmentation pathways of phthalate esters by gas chromatography–tandem mass spectrometry. **2014,** *47* (9), 1579-1588.
45. Cone, C.; Dewar, M. J.; Landman, D. J. J. o. t. A. C. S., Gaseous ions. 1. MINDO/3 study of the rearrangement of benzyl cation to tropylium. **1977,** *99* (2), 372-376.
46. Rylander, P. N.; Meyerson, S.; Grubb, H. M. J. J. o. t. A. C. S., Organic ions in the gas phase. II. The tropylium ion. **1957,** *79* (4), 842-846.
47. Capozzi, V.; Yener, S.; Khomenko, I.; Farneti, B.; Cappellin, L.; Gasperi, F.; Scampicchio, M.; Biasioli, F. J. J., PTR-ToF-MS coupled with an automated sampling system and tailored data analysis for food studies: bioprocess monitoring, screening and nose-space analysis. **2017,** (123), e54075.